Corrections

GENETICS. For the article "Genome analysis of multiple pathogenic isolates of *Streptococcus agalactiae*: Implications for the microbial 'pan-genome'," by Hervé Tettelin, Vega Masignani, Michael J. Cieslewicz, Claudio Donati, Duccio Medini, Naomi L. Ward, Samuel V. Angiuoli, Jonathan Crabtree, Amanda L. Jones, A. Scott Durkin, Robert T. DeBoy, Tanja M. Davidsen, Marirosa Mora, Maria Scarselli, Immaculada Margarit y Ros, Jeremy D. Peterson, Christopher R. Hauser, Jaideep P. Sundaram, William C. Nelson, Ramana Madupu, Lauren M. Brinkac, Robert J. Dodson, Mary J. Rosovitz, Steven A. Sullivan, Sean C. Daugherty, Daniel H. Haft, Jeremy Selengut, Michelle L. Gwinn, Liwei Zhou, Nikhat Zafar, Hoda Khouri, Diana Radune, George Dimitrov, Kisha Watkins, Kevin J. B. O'Connor, Shannon Smith, Teresa R. Utterback, Owen White, Craig E. Rubens, Guido Grandi, Lawrence C. Madoff, Dennis L. Kasper, John L. Telford, Michael R. Wessels, Rino Rappuoli, and Claire M. Fraser, which appeared in issue 39, September 27, 2005, of *Proc. Natl. Acad. Sci. USA* (**102,** 13950–13955; first published September 19, 2005; 10.1073/pnas.0506758102), the authors note that gene designations appeared incorrectly. On page 13954, in the left column under *Origin of Genomic Islands and Strain-Specific Genes*, the last two sentences of the second paragraph read as follows:

"Of these proteins, COH1_ORF01523 corresponds to adhesin Spb1, a serotype III-specific protein implicated in adhesion and invasion of epithelial cells (26), whereas the other two (COH1_ORF01521 and COH1_ORF01524) are similar to a fimbrial subunit and to internalin A of *Listeria monocytogenes*, respectively. Another region shared by strain H36B and *S. pneumoniae* contains an α-galactosidase (H36B_ORF00495) and a system for transport and metabolism of sugar that may allow H36B to degrade and transport host α-galactosides."

The sentences should read as follows:

"Of these proteins, SAN_1518 corresponds to adhesin Spb1, a serotype III-specific protein implicated in adhesion and invasion of epithelial cells (26), whereas the other two (SAN_1516 and SAN_1519) are similar to a fimbrial subunit and to internalin A of *Listeria monocytogenes*, respectively. Another region shared by strain H36B and *S. pneumoniae* contains an α-galactosidase (SAL_0496) and a system for transport and metabolism of sugar that may allow H36B to degrade and transport host α-galactosides."

In addition, the second sentence of the last paragraph of that same section, "For example, type Ib isolate H36B contains a 41-kb prophage element (H36B_ORF00576–H36B_ORF00630) that displays strong mosaicism and contains a protein (H36B_ORF00630) similar to the *S. pyogenes* phage-associated pyrogenic exotoxin C," should read: "For example, type Ib isolate H36B contains a 41-kb prophage element (SAL_0571–SAL_0626) that displays strong mosaicism and contains a protein (SAL_0626) similar to the *S. pyogenes* phage-associated pyrogenic exotoxin C." These changes do not alter the conclusions of the article.

www.pnas.org/cgi/doi/10.1073/pnas.0508532102

MEDICAL SCIENCES. For the article "Differential responses to psychotherapy versus pharmacotherapy in patients with chronic forms of major depression and childhood trauma," by Charles B. Nemeroff, Christine M. Heim, Michael E. Thase, Daniel N. Klein, A. John Rush, Alan F. Schatzberg, Philip T. Ninan, James P. McCullough, Jr., Paul M. Weiss, David L. Dunner, Barbara O. Rothbaum, Susan Kornstein, Gabor Keitner, and Martin B. Keller, which appeared in issue 24, November 25, 2003, of *Proc. Natl. Acad. Sci. USA* (**100,** 14293–14296; first published November 13, 2003; 10.1073/pnas.2336126100), the authors note the following. "Results of the analyses of variance comparing change in Hamilton Rating Scale for Depression scores as a function of treatment type and early life trauma histories as well as Fig. 1*A* reflect change relative to the *first* week of treatment instead of baseline. When change scores relative to baseline are used, the interaction effects between treatment type and childhood trauma histories are not statistically significant. This discrepancy is due to marked changes in depression scores during the first week of treatment. Note that all analyses comparing the more conservative outcome measure of remission as a function of treatment type and childhood trauma as well as Fig. 1*B* are correct. Thus, consideration of treatment response relative to baseline does not detect the effect of childhood trauma on final remission, whereas consideration of final response relative to first response does detect the effect."

www.pnas.org/cgi/doi/10.1073/pnas.0508675102

NEUROSCIENCE. For the article "Unraveling a role for dopamine in Huntington's disease: The dual role of reactive oxygen species and D2 receptor stimulation," by Delphine Charvin, Peter Vanhoutte, Christiane Pagès, Emiliana Borelli, and Jocelyne Caboche, which appeared in issue 34, August 23, 2005, of *Proc. Natl. Acad. Sci. USA* (**102,** 12218–12223; first published August 15, 2005; 10.1073/pnas.0502698102), the author name Emiliana Borelli should have appeared as Emilliana Borrelli. The corrected author line appears below. The online version has been corrected.

Delphine Charvin, Peter Vanhoutte, Christiane Pagès, Emilliana Borrelli, and Jocelyne Caboche

www.pnas.org/cgi/doi/10.1073/pnas.0508079102

Unraveling a role for dopamine in Huntington's disease: The dual role of reactive oxygen species and D2 receptor stimulation

Delphine Charvin*, Peter Vanhoutte*, Christiane Pagès*, Emilliana Borrelli†, and Jocelyne Caboche*‡

*Unité Mixte de Recherche 7102, Signalisation Neuronale et Régulations Géniques, 9 Quai Saint Bernard, 75005 Paris, France; and †Institut de Génétique et de Biologie Moléculaire et Cellulaire, 1 Rue L. Fries, 67404 Illkirch Cedex, France

Huntington's disease (HD), an inherited neurodegenerative disorder, results from an abnormal polyglutamine extension in the N-terminal region of the huntingtin protein. This mutation leads to protein aggregation and neurotoxicity. Despite its widespread expression in the brain and body, mutated huntingtin causes selective degeneration of striatal projection neurons. In the present study, we investigate the role of dopamine (DA) in this preferential vulnerability. Using primary cultures of striatal neurons transiently expressing GFP-tagged-exon 1 of mutated huntingtin, we show that low doses of DA (100 μM) act synergistically with mutated huntingtin to activate the proapoptotic transcription factor c-Jun. Surprisingly, DA also increases aggregate formation of mutated huntingtin in all cellular compartments, including neurites, soma, and nuclei. DA-dependent potentiation of c-Jun activation was reversed by ascorbate, a reactive oxygen species (ROS) scavenger, and SP-600125, a selective inhibitor of the c-Jun N-terminal kinase (JNK) pathway. By contrast, DA effects on aggregate formation were reversed by a selective D2 receptor antagonist and reproduced by a D2 agonist. Similarly, striatal neurons from D2 knockout mice showed no effect of DA on aggregate formation. Blocking ROS production, JNK activation, or D2 receptor stimulation significantly reversed DA aggravation of mutated huntingtin-induced striatal death. The combined treatment with the ROS scavenger and D2 antagonist totally reversed DA's effects on mutated huntingtin-induced striatal death. Thus, the present results provide insights into the cellular mechanisms that govern striatal vulnerability in HD and strongly support a dual role of JNK activation and D2 receptor signaling in this process.

aggregates | expanded huntingtin | c-Jun N-terminal kinase

Huntington's disease (HD) is a neurodegenerative disorder characterized by chorea, psychiatric disturbances, and cognitive impairment (1). This autosomal, dominant, inherited disorder results from an abnormal CAG repeat expansion in exon 1 of the *HD* gene, which is translated into an abnormally long polyglutamine tract at the N terminus of the huntingtin protein (Htt) (2). Htt is a 350-kDa protein of unknown function that is essential for normal embryonic development and neurogenesis (3). Cleavage of expanded huntingtin (expHtt) leads to the release of N-terminal fragments containing the polyglutamine repeats. These fragments accumulate and form intraneuronal aggregates in neurites, cytoplasm, and nuclei (4–6). The pathogenic role of these aggregates in the disease remains controversial, but they are a common hallmark of numerous neurodegenerative disorders (7).

Selective neurodegeneration in the patient brain, which occurs most prominently in the striatum, constitutes the basis of the neurological symptoms of HD (8). Despite the widespread expression of Htt in the brain and body, medium-size spiny GABAergic neurons of the striatum are preferentially affected in HD. This specific neurodegeneration is important in the pathophysiology of the disease because the evolution and severity of the symptoms are directly correlated to the rate of caudate atrophy (9). The striatum receives the densest dopaminergic innervation of the brain, and HD progresses according to a striatal dorsoventral gradient corresponding to the gradient of dopamine (DA) concentration (10). Thus, the physiological DA release that occurs in the striatum during the normal life span could participate in the preferential and progressive vulnerability of striatal neurons in HD. Although numerous indirect arguments suggest a role of DA in HD (11), the precise mechanism by which DA could aggravate mutated huntingtin toxicity remains to be elucidated.

In the present study, we show that low doses of DA aggravate expHtt-induced neuronal death via two distinct routes. One route involves activation of the proapoptotic c-Jun N-terminal kinase (JNK)/c-Jun pathway by oxidative stress, and the other route involves the stimulation of dopaminergic D2 receptor. Thus, our study provides insights into the cellular mechanisms that make striatal neurons more vulnerable to toxicity induced by expHtt and strongly supports a prominent role of DA in the specificity of cell death in HD.
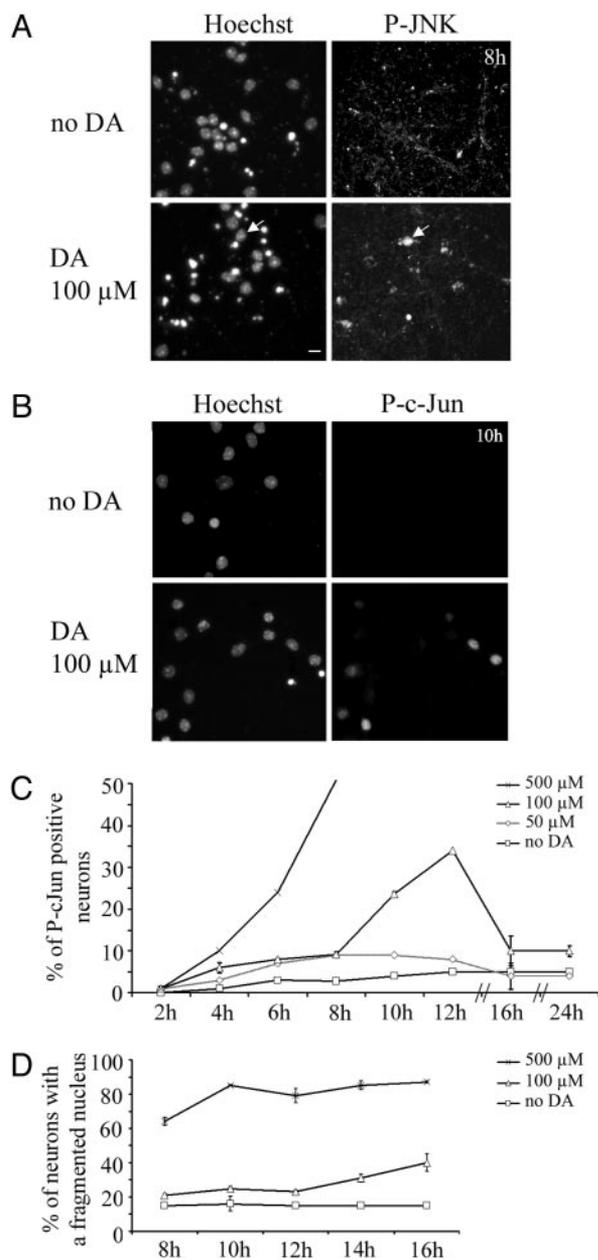
Methods

Embryos were removed at day 14 from timed-pregnant Swiss mice (Janvier, Le Genest-St-Isle, France) or D2 receptor knockout mice. Striatal cultures and transfections were performed as described in ref. 12. cDNAs for Htt and expHtt (provided by the Huntington's Disease Foundation Resource Bank, University of California, Los Angeles) correspond to pcDNA3 containing the CMV promoter controlling the expression of the entire exon 1 of the human *huntingtin* gene (*IT15*), with 25 (Htt) or 103 (expHtt) continuous CAA or CAG repeats. A sequence encoding an EGFP was inserted in frame at the C terminus of each construct. In parallel, the coding sequence of the *EGFP* gene was expressed under the control of the CMV promoter (referred to as GFP). Four hours after transfection, the medium was removed and replaced by the complete neurobasal medium containing DA (Calbiochem) or quinpirole (Research Biochemicals, Natick, MA), then cells were replaced at 37°C for the appropriate time. For the pharmacological treatments, 10 μM SCH-23390 (Sigma), 1 μM raclopride (Sigma), 200 μM ascorbate (Aldrich), or 20 μM SP-600125 (Calbiochem) was added 30 min before and during DA treatment. For immunofluorescence, cells were incubated with monoclonal anti-microtubule-associated protein 2 (anti-MAP2) at 1:100 [kindly provided by B. Riederer (Institut d'Anatomie, Lausanne, Switzerland)] and polyclonal anti-phospho Ser-73 c-Jun at 1:500 (Ozyme, Saint Quentin Yvelines, France) and then with the appropriate secondary

A   Hoechst   P-JNK

no DA

DA
100 μM

B   Hoechst   P-c-Jun

no DA

DA
100 μM

C
% of P-cJun positive neurons

— 500 μM
— 100 μM
— 50 μM
— no DA

D
% of neurons with a fragmented nucleus

— 500 μM
— 100 μM
— no DA

Fig. 1. DA activates the JNK/c-Jun pathway in striatal neurons. (*A* and *B*) Activation of JNK (*A*) and c-Jun (*B*) by 100 μM DA was detected by using antibodies selective for activated phosphorylated JNK (P-JNK) and P-c-Jun, respectively. (Scale bar, 10 μm.) (*A*) Note the nuclear translocation of P-JNK upon DA treatment (arrow). (*C* and *D*) The kinetics of c-Jun activation (*C*) and striatal death determined by a fragmented nucleus (*D*) induced by different doses of DA in striatal neurons. The percentages were calculated with an image analysis software (IMAGE PRO PLUS). Data are representative of three independent experiments for each dose (50, 100, or 500 μM) and time point (from 2 to 24 h) of DA exposure.

antibody: (Cy3)-conjugated anti-rabbit IgG at 1:2,000 (Amersham Pharmacia) or (Cy3)-conjugated anti-mouse IgG at 1:2,000 (The Jackson Laboratory). For double labeling, anti-*p*-c-Jun and anti-MAP2 antibodies were revealed with a (Cy3)-conjugated anti-rabbit IgG and a biotinylated horse anti-mouse IgG at 1:100 (Vector Laboratories), respectively. Cells were observed under a Leica DM LB fluorescence microscope. Neurons containing condensed or fragmented nuclei (DNA labeling with Hoechst) were scored as dying cells. For each condition, a minimum of 600
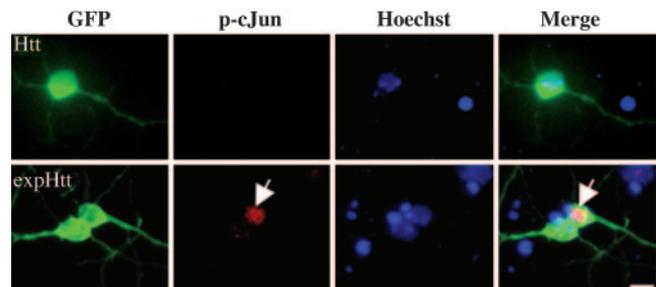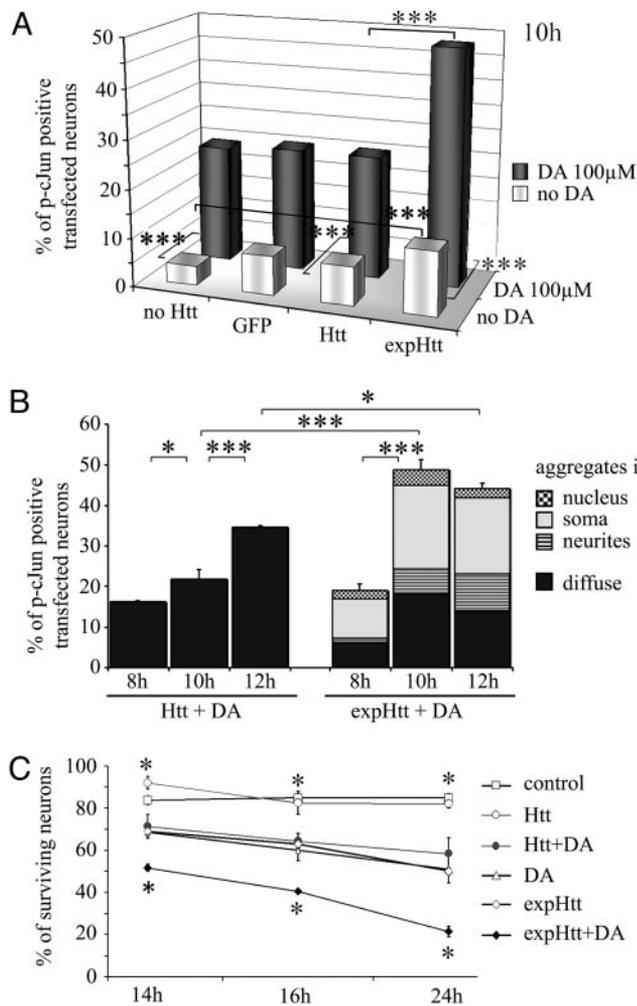

Fig. 2. ExpHtt activates the proapoptotic c-Jun transcription factor. GFP–Htt (Htt) or GFP–expHtt (expHtt) were transiently transfected into striatal neurons and visualized by GFP expression. Activation of c-Jun was detected by using an anti-phospho-c-Jun (*p*-cJun) antibody (red labeling) in the nucleus (Hoechst, blue staining) of striatal neurons transfected with expHtt (arrow).

transfected neurons were counted from three independent experiments. Phosphorylated c-Jun (P-c-Jun) immunoreactivity was quantified with the image analysis software IMAGE PRO PLUS 4.5.0.19 (Media Cybernetics, Silver Spring, MD). Results were compared by using ANOVA between subjects, and post hoc comparisons were made by using the indicated test (see Figs. 3–5). Detailed procedures and reagents are described in *Supporting Methods*, which is published as supporting information on the PNAS web site.
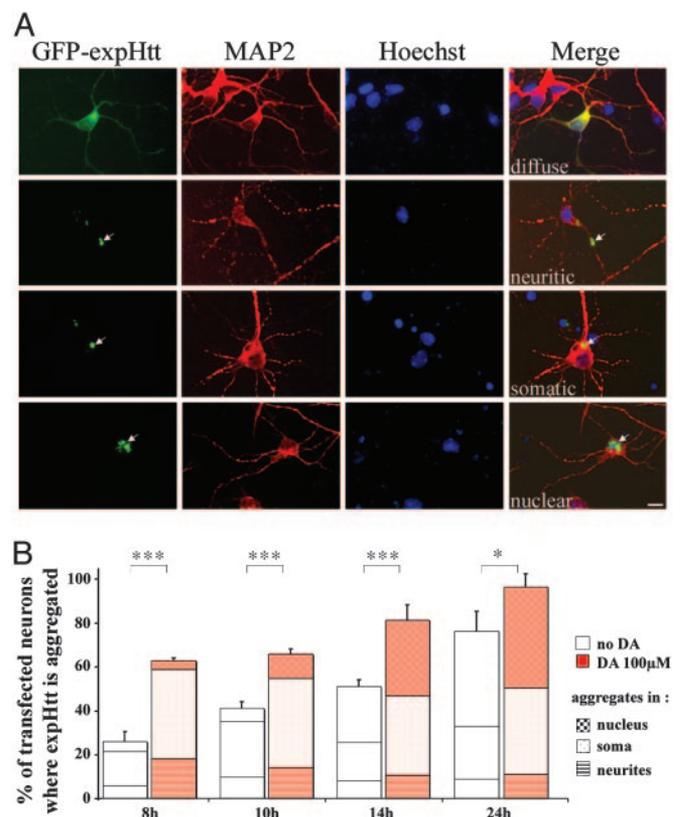
Results

DA Activates the JNK/c-Jun Pathway in Striatal Neurons in a Time- and Dose-Dependent Manner. High doses of DA are known to induce striatal death *in vitro* and *in vivo* (11). To investigate the presence of a possible synergism between DA and expHtt fragments, we first analyzed the kinetics and dose–response effects of DA on cultures of primary striatal neurons. Two parameters were taken into account: activation of the proapoptotic JNK/c-Jun pathway (13) and neuronal death. In our conditions, primary striatal cultures were completely devoid of DAergic neurons as proved by the total lack of tyrosine hydroxylase expression (Fig. 6*A*, which is published as supporting information on the PNAS web site). Activation of JNK and c-Jun was analyzed by immunocytochemistry using antibodies that specifically recognize their active, phosphorylated form (14). Fig. 1 *A* and *B* illustrate phosphorylated JNK and P-c-Jun immunoreactivities after 8 and 10 h of 100 μM DA treatment, respectively. Increasing concentrations of DA (50 μM, 100 μM, and 500 μM) were applied on striatal cultures. c-Jun phosphorylation occurred in a time- and concentration-dependent manner (Fig. 1*C*). At 500 μM DA, c-Jun phosphorylation was very rapid and high (>50% of c-Jun-positive striatal neurons at 8 h) and unobservable later on because of significant striatal death (see Fig. 1*D*). In response to 100 μM DA, c-Jun activation occurred more slowly and transiently, reaching a maximum (up to 7-fold when compared with controls) at 12 h and returning to control values by 16 h (Fig. 1*C*). c-Jun activation occurred subsequently to nuclear translocation of activated JNK (Fig. 1*A*). No significant activation of c-Jun was found with 50 μM DA (Fig. 1*C*).

The kinetics of striatal death by DA was determined by evaluating nuclear integrity (as determined by Hoechst staining). Whereas DA applied at 500 μM induced a strong and rapid striatal death, this effect was more progressive and modest when cells were challenged with 100 μM DA, with 60% of living striatal neurons at 16 h (Fig. 1*D*). Based on these data, 100 μM DA (i.e., the lowest DA concentration allowing detection of c-Jun activation) was used in further experiments at time points when little or no effects could be detected on striatal neuron death (from 8 to 12 h).

NEUROSCIENCE

Fig. 3. DA potentiates expHtt-induced c-Jun activation and neuronal death. (*A*) Comparative effects of 100 μM DA (at 10 h) on c-Jun activation in striatal neurons that were not transfected (no Htt) or transfected with GFP alone (GFP), normal Htt (Htt), or mutated Htt (expHtt). Gray bars, without DA; black bars, with DA. Data are representative of three independent experiments for each condition and each time point (100 cells counted per well; two wells per experiment; 600 transfected cells for each condition). Statistical analyses were performed using ANOVA followed by Fisher's analysis for post hoc comparisons: ***, $P < 0.001$. (*B*) Kinetics (at 8, 10, and 12 h) of c-Jun activation in Htt- or expHtt- transfected neurons in the presence of 100 μM DA. Different populations of P-c-Jun-positive neurons were separated on the basis of GFP–expHtt localization, i.e., diffuse or aggregated in the neurites, soma, or nucleus. *, $P < 0.05$; ***, $P < 0.001$. (*C*) Kinetics (at 14, 16, and 24 h) of DA effects on survival of striatal neurons in control conditions or after transfection (Htt or expHtt). The percentage of surviving neurons was determined by morphological criteria based on DNA labeling with Hoechst. Quantification and statistical analyses were performed as in *A*. *, $P < 0.05$ when compared with expHtt.
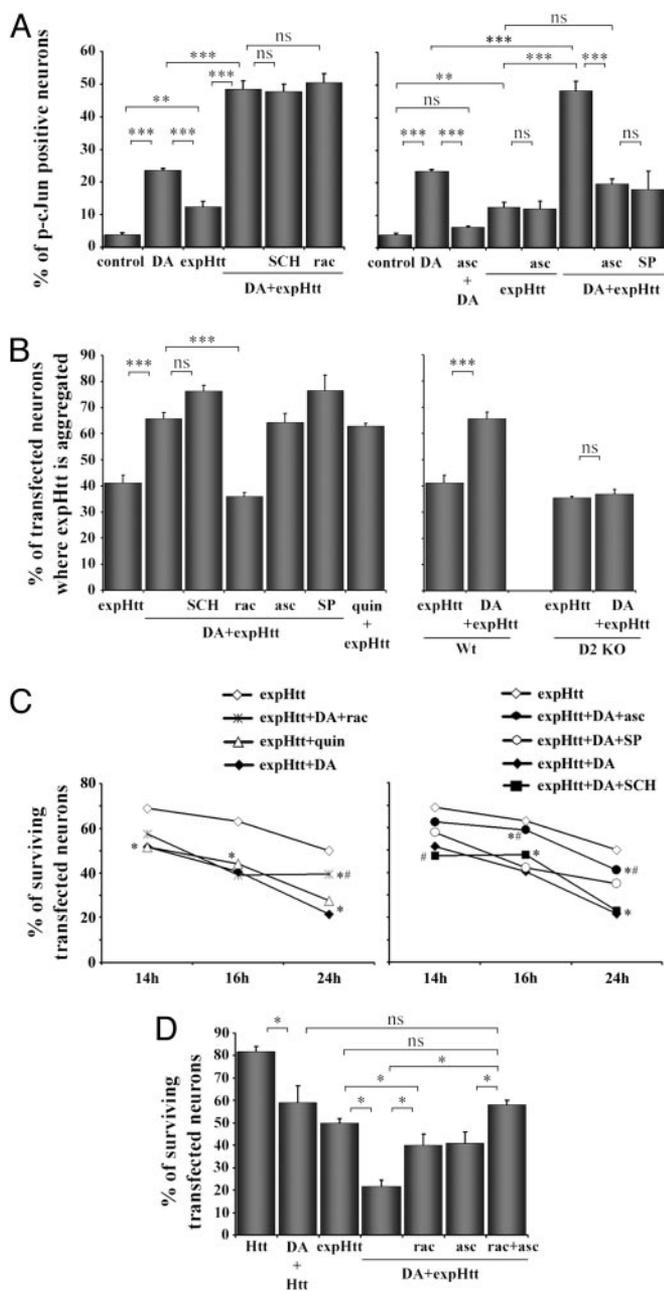
DA Potentiates c-Jun Activation and Striatal Death Induced by Expanded Htt. Next, we analyzed the combined effect of DA and expHtt on c-Jun activation in striatal neurons. c-Jun activation was analyzed as described above, in striatal neurons expressing either normal Htt or the mutated form, expHtt (Fig. 2). As described in ref. 12, expHtt but not Htt activated c-Jun in striatal neurons, but this activation remained an early (8 h after transfection) and modest (15% of expHtt-transfected neurons) event (Fig. 6*B*). When DA (100 μM) was combined with the transient expression of Htt, c-Jun activation was increased to similar proportions than DA alone or DA applied on GFP-transfected neurons (Fig. 3*A*). However, at this dose, DA produced a clear

Fig. 4. DA increases aggregate formation of expHtt. (*A*) GFP-tagged expHtt localizations at 10 h. Neuronal compartments were defined by using immunolabeling of MAP2 (in red) for neurites and soma and Hoechst staining (in blue) for the nucleus. Merge represents the combined image of MAP2, Hoechst, and GFP. Note the four different patterns at this time point: diffuse or present in neuritic, somatic, or nuclear aggregates (arrows). (Scale bar, 10 μm.) (*B*) Effect of DA on expHtt aggregate formation at different time points after transfection (8, 10, 14, and 24 h). ANOVA revealed significant differences in aggregate formation of expHtt when neurons were treated with 100 μM DA (compare for each time point: left column in each column pair, no DA; right column in each column pair, 100 μM DA). For each time point, the number of transfected neurons where expHtt is aggregated is significantly higher in the presence of 100 μM DA (right column in each column pair) (Fisher's analysis; ***, $P < 0.001$; *, $P < 0.05$).

synergistic effect on c-Jun phosphorylation in expHtt-expressing neurons, with 50% of expHtt expressing striatal neurons instead of 25% and 13% for DA or expHtt alone, respectively (Fig. 3*A*). c-Jun potentiation by DA occurred at 10 h (Fig. 3*B*), i.e., after expHtt induced effects (see Fig. 6*B*).

Consistent with its potentiating role on c-Jun activation, DA also aggravated expHtt-induced striatal death (at 24 h, 20% of surviving neurons when compared with 50% in the absence of DA) (Fig. 3*C*), whereas DA application on Htt-expressing neurons induced striatal death to the same level as DA alone (Fig. 3*C*).

DA Increases expHtt-Induced Aggregate Formation. The presence of a GFP tag at the C-terminal region of expHtt allowed us to follow its subcellular localization and aggregate formation. Various patterns of expHtt localization were found at the different time points after transfection. This finding is well illustrated in Fig. 4*A*, where the triple labeling with Hoechst, the MAP2 (a neuritic marker) immunostaining, and the GFP fusion to expHtt identify distinct labeling patterns (shown here at 10 h after transfection): a diffuse GFP labeling or labeling in neuritic, somatic, or nuclear aggregates.

Charvin *et al.*

Fig. 5. DA potentiates c-Jun activation, aggregate formation, and neuronal death induced by expHtt effects via distinct pathways. (*A*) Pharmacological characterization of DA effects on c-Jun activation by expHtt. P-c-Jun immunoreactive neurons were quantified at 10 h in control, DA-treated (100 μM) (DA), or expHtt-transfected neurons. (*Left*) DA was applied in expHtt-transfected neurons (DA+expHtt) alone or in the presence of a selective D1 (10 μM SCH23390; SCH) or D2 (1 μM raclopride; rac) antagonist. (*Right*) The ROS scavenger (200 μM ascorbate; asc) and the selective JNK inhibitor (20 μM SP-600125; SP) were applied in expHtt-transfected neurons alone (expHtt) or in the presence of DA (DA+expHtt). (*B*) Pharmacological characterization of DA effects on expHtt aggregate formation. (*Left*) The experimental procedures for the pharmacological studies were the same as in *A*. The D2 agonist quinpirole (quin) was applied at 10 μM. (*Right*) Effect of DA on expHtt aggregate formation in striatal neurons from wild-type (Wt) or D2 receptor knockout (D2 KO) mice. (*A* and *B*) Quantifications were performed as indicated in Fig. 3. Statistical analyses: ***, *P* < 0.001; **, *P* < 0.005; ns, nonsignificant (Bonferroni/Dunnet's analysis). (*C*) Role of DA on survival of expHtt-expressing striatal neurons. The pharmacological treatments are the same as in *A* and *B*. ExpHtt-transfected neurons were analyzed for their nuclear integrity by Hoechst staining at 14, 16, and 24 h. *, *P* < 0.05 when compared with expHtt; #, *P* < 0.05 when compared with expHtt plus DA. (*D*) A cotreat-

Few cells showed expHtt aggregates at 8 h (25%) (Fig. 4*B*). Later on, aggregates progressively increased reaching ≈80% of expHtt-expressing neurons at 24 h, a time when the majority of aggregates were nuclear. Surprisingly, a strong and early potentiation of expHtt aggregates was found in the presence of DA. At 8 h, DA induced expHtt aggregate formation in 65% of striatal neurons (when compared with 25% without DA; see Fig. 4*B*). This effect was persistent, given that at 24 h 97% of expHtt-expressing neurons showed aggregates in the presence of DA, compared with 77% without DA.

DA Plays a Dual Role on expHtt-Induced Phenotype in Striatal Neurons. Our results clearly show a potentiating role of DA on three important aspects of expHtt-induced phenotype in striatal neurons: c-Jun activation, aggregate formation, and striatal death. DA can act on striatal neurons through two distinct receptors, the D1 and D2 receptors, which can be distinguished on the basis of intracellular signaling (i.e., stimulation and inhibition of adenylate cyclase activity, respectively). DA effects on the expHtt-induced phenotype might also reflect its neurotoxicity by oxidative metabolism, because DA can oxidize spontaneously *in vitro* or through an enzyme-catalyzed reaction *in vivo* to form reactive oxygen species (ROS) (15). We therefore investigated the respective role of D1/D2 receptor stimulation and ROS production on expHtt-induced phenotype. Treatments with dopaminergic antagonists (D1 or D2) or inhibitors (ROS scavenger or JNK inhibitor) were combined with DA.

Although neither D1- nor D2-selective antagonists (SCH-23390 and raclopride, respectively) had any effect on DA potentiation of c-Jun activation by expHtt (Fig. 5*A Left*), ascorbate (ROS scavenger) totally blocked this effect (Fig. 5*A Right*). Ascorbate also inhibited c-Jun activation induced by DA alone but had no effect on c-Jun activation induced by expHtt alone, indicating that expHtt induces c-Jun activation independently of ROS production. Similarly to ascorbate, SP-600125, a selective JNK inhibitor, blocked the synergistic effect of DA and expHtt on c-Jun activation. Thus, altogether these results strongly support that the synergistic effect of DA and expHtt on c-Jun activation is mediated by JNK activation via ROS production.

Next, we analyzed how DA potentiates expHtt aggregate formation. Although we found no effect of the D1 antagonist or the ROS or JNK inhibitors (Fig. 5*B*), DA effects on aggregate formation were totally blocked by a selective D2 antagonist and mimicked by a D2 agonist (Fig. 5*B Left*). Importantly, primary striatal neurons from D2 knockout mice (16) showed no DA potentiation of expHtt aggregate formation (Fig. 5*B Right*). Thus, these data provide evidence that D2 receptors stimulation can induce expHtt aggregate formation in striatal neurons.

Finally, we examined the respective influence of D1/D2 receptor stimulation and ROS production or JNK activation on DA aggravation of expHtt-induced neuronal death (Fig. 5 *C* and *D*). This influence was examined at different time points after DA treatment. The greatest effects were visible at 24 h when DA strongly reduced survival in expHtt-expressing striatal neurons (20% versus 50% of surviving neurons when comparing expHtt plus DA with expHtt alone). Whereas the D2 antagonist, raclopride, significantly reversed DA effects on expHtt-induced neuronal death, the D2 agonist, quinpirole, reproduced these effects (Fig. 5*C Left*). It is important to note that quinpirole alone had no effect on striatal survival (93% of surviving neurons after 24h treatment. Data not shown). The D1 antagonist was devoid of effect on DA-mediated expHtt-induced

ment with ROS scavenger (200 μM ascorbate) and D2 antagonist (1 μM raclopride) is more protective for expHtt-expressing neurons exposed to 100 μM DA (at 24 h) than each simple treatment with ascorbate or raclopride. (*, *P* < 0.05; ns, nonsignificant; Fisher's test post ANOVA.)

NEUROSCIENCE

neuronal death, but the ROS scavenger (ascorbate) and the JNK inhibitor (SP-600125) significantly reversed DA potentiation of expHtt-induced neuronal death (40% versus 20% of surviving neurons) (Fig. 5C Right). We note that ascorbate had no effect on striatal death induced by expHtt alone (data not shown), a data consistent with its lack of effect on expHtt-induced c-Jun activation (see Fig. 5A). Importantly, a cotreatment with the ROS scavenger and D2 antagonist totally protected neurons against the combined toxicity of DA and expHtt (Fig. 5D).

Discussion

Our data show that DA aggravates expHtt toxicity in striatal neurons not only through the production of ROS, which activate the proapoptotic JNK/c-Jun pathway, but also by D2 receptor stimulation, which increases aggregate formation.

Activation of the proapoptotic JNK/c-Jun pathway contribute to the neuronal atrophy and death that can be observed in neurodegenerative diseases, including Alzheimer's and Parkinson's disease, and in pathological conditions, such as stroke (17). In in vitro models of HD, such as expHtt overexpression in hippocampal cell lines or primary striatal neurons in culture, expHtt can activate the JNK/c-Jun pathway independently of ROS production (12, 18–20). Here we provide evidence that DA is implicated in a synergistic manner with expHtt to activate c-Jun in striatal neurons. DA can autooxidize and form ROS that were shown in other systems to be important for cell death (21). DA-induced ROS production is known to activate the JNK/c-Jun pathway, and blocking this pathway enables the reversal of DA-induced cell death (15). Our data showing a synergistic effect of DA and expHtt on c-Jun activation are of critical relevance for HD and striatal vulnerability. Thus, the increased autooxidation of DA that occurs in the striatum during aging (22) could potentiate a low level of JNK/c-Jun activation that is due to expHtt expression (12, 17, 19). This process could account for a selective vulnerability of striatal neurons toward this proapoptotic signaling pathway. Autooxidation of DA during aging could also explain why the onset of symptoms and degeneration is delayed to adulthood, despite the constitutive expression of expHtt mutation since birth.

DA treatment also accelerated the kinetics of expHtt aggregate formation through D2 receptors, which demonstrates that an extracellular stimulation can influence expHtt aggregate formation. In presymptomatic HD patients, the first brain areas in which neuropil aggregates appear are the globus pallidus and the substantia nigra (23), two brain regions where D2 receptors are concentrated (24, 25). D2 receptors are also strongly expressed by medium spiny neurons, and more particularly by GABAergic/enkephalinergic neurons (26), which represent the first striatal population affected in HD (27, 28). Thus, our data help to reconcile these neuroanatomical observations and strongly argue for a role of D2 receptor stimulation in aggregate formation as an early event in HD.

There is still a strong debate about the role of aggregates in neurotoxicity. Aggregates of expHtt are observed in HD postmortem patients' brains as well as in different animal models of HD (6, 29–32), in which they typically precede an onset of symptoms (23, 33). These aggregates are associated with axonal degeneration as an early pathological event in mice with HD (23), and within the nucleus they are thought to inhibit transcriptional events that are important for the expression of antiapoptotic genes (34, 35). More recently, aggregates of expHtt were proposed to interfere with the proteasome function (36), which is important for the clearance of toxic proteins. Arrasate et al. (37) also provided convincing data about the neuroprotective role of aggregates, at least in early stages, because striatal neurons that contained aggregates had a decreased cumulative risk of death when compared with diffused expHtt. Whether D2-mediated aggregates are a cause or a consequence of expHtt toxicity remains to be established. However, we propose that the increased formation of aggregates in response to D2 receptors is a signature of the greater sensitivity of this striatal subpopulation to expHtt.

DA increased expHtt-induced striatal death, a finding strongly arguing for a pathogenic role of DA in the selective vulnerability of striatal neurons in HD. This role was already suggested from pharmacological models of HD in which removal of the nigrostriatal dopaminergic input protected the striatum from neurodegeneration induced by these toxins (38, 39). Furthermore, subtoxic doses of 3-NP produce striatal neurodegeneration when combined with a subtoxic dose of methamphetamine (40). In DA transporter knockout mice, spontaneous striatal death accompanied by behavioral alterations that resemble HD are observed during aging specifically (41). No direct link between DA toxicity and HD mutation has been shown from in vivo genetic mice models of HD. However, in vitro, striatal neurons derived from the R6/2 mice are more susceptible than wild-type cells to high and neurotoxic concentrations (1 mM) of DA (42). In our model system, we have been able to unravel two fundamental events involved in the death pathway produced by lower doses of DA (100 μM). The first pathway is c-Jun activation by ROS, and the second is D2 receptor stimulation, which in turn increases aggregate formation. Noteworthy, these two DA-mediated events occurred early in the pathogenic process induced by expHtt. Thus, blocking at presymptomatic stages of the disease, JNK activation, and D2 receptor-mediated signaling might represent promising strategies for HD therapy. These strategies are important considering that, so far, there are no available therapies aimed at slowing down disease progression, and, consequently, HD progresses inexorably to death. Although most of the patients are treated by neuroleptics that share D2 receptor antagonist properties, there is no clear correlation between neuroleptic treatments and rate of illness progression (43, 44). Furthermore, patients who receive neuroleptics may experience numerous side effects, including extrapyramidal syndrome. Elucidating the nature of elements participating in the signaling pathways involved in neurodegeneration downstream of the D2 receptor might lead to the development of novel therapeutical targets. It may help to design better tolerated drugs that could be given to presymptomatic patients as a therapeutic option aimed at forestalling the onset of the disease.

1. Krawczak, M., Bockel, B., Sandkuijl, L., Thies, U., Fenton, I. & Harper, P. S. (1991) Am. J. Hum. Genet. 49, 735–745.
2. The Huntington's Disease Collaborative Research Group (1993) Cell 72, 971–983.
3. Dragatsis, I., Levine, M. S. & Zeitlin, S. (2000) Nat. Genet. 26, 300–306.
4. Mangiarini, L., Sathasivam, K., Seller, M., Cozens, B., Harper, A., Hetherington, C., Lawton, M., Trottier, Y., Lehrach, H., Davies, S. W. & Bates, G. P. (1996) Cell 87, 493–506.
5. Davies, S. W., Turmaine, M., Cozens, B. A., DiFiglia, M., Sharp, A. H., Ross, C. A., Scherzinger, E., Wanker, E. E., Mangiarini, L. & Bates, G. P. (1997) Cell 90, 537–548.
6. DiFiglia, M., Sapp, E., Chase, K. O., Davies, S. W., Bates, G. P., Vonsattel, J. P. & Aronin, N. (1997) Science 277, 1990–1993.
7. Trojanowski, J. Q. & Lee, V. M. (2000) Ann. N.Y. Acad. Sci. 924, 62–67.
8. Vonsattel, J. P., Myers, R. H., Stevens, T. J., Ferrante, R. J., Bird, E. D. & Richardson, E. P., Jr. (1985) J. Neuropathol. Exp. Neurol. 44, 559–577.
9. Aylward, E. H., Codori, A. M., Rosenblatt, A., Sherr, M., Brandt, J., Stine, O. C., Barta, P. E., Pearlson, G. D. & Ross, C. A. (2000) Movement Disord. 15, 552–560.
10. Cass, W. A. (1997) J. Pharmacol. Exp. Ther. 280, 105–113.
11. Jakel, R. J. & Maragos, W. F. (2000) Trends Neurosci. 23, 239–245.
12. Garcia, M., Charvin, D. & Caboche, J. (2004) Neuroscience 127, 859–870.
13. Wang, L. H., Besirli, C. G. & Johnson, E. M., Jr. (2004) Annu. Rev. Pharmacol. Toxicol. 44, 451–474.
14. Willaime-Morawek, S., Brami-Cherrier, K., Mariani, J., Caboche, J. & Brugg, B. (2003) Neuroscience 119, 387–397.

15. Luo, Y., Umegaki, H., Wang, X., Abe, R. & Roth, G. S. (1998) *J. Biol. Chem.* **273,** 3756–3764.
16. Baik, J. H., Picetti, R., Saiardi, A., Thiriet, G., Dierich, A., Depaulis, A., Le Meur, M. & Borrelli, E. (1995) *Nature* **377,** 424–428.
17. Bozyczko-Coyne, D., Saporito, M. S. & Hudkins, R. L. (2002) *Curr. Drug Targets CNS Neurol. Disord.* **1,** 31–49.
18. Liu, Y. F. (1998) *J. Biol. Chem.* **273,** 28873–28877.
19. Liu, Y. F., Dorow, D. & Marshall, J. (2000) *J. Biol. Chem.* **275,** 19035–19040.
20. Merienne, K., Helmlinger, D., Perkin, G. R., Devys, D. & Trottier, Y. (2003) *J. Biol. Chem.* **278,** 16957–16967.
21. McLaughlin, B. A., Nelson, D., Erecinska, M. & Chesselet, M. F. (1998) *J. Neurochem.* **70,** 2406–2415.
22. Fornstedt, B., Pileblad, E. & Carlsson, A. (1990) *J. Neurochem.* **55,** 655–659.
23. Li, H., Li, S. H., Yu, Z. X., Shelbourne, P. & Li, X. J. (2001) *J. Neurosci.* **21,** 8473–8481.
24. Floran, B., Floran, L., Sierra, A. & Aceves, J. (1997) *Neurosci. Lett.* **237,** 1–4.
25. Cooper, A. J. & Stanford, I. M. (2001) *Neuropharmacology* **41,** 62–71.
26. Missale, C., Nash, S. R., Robinson, S. W., Jaber, M. & Caron, M. G. (1998) *Physiol. Rev.* **78,** 189–225.
27. Reiner, A., Albin, R. L., Anderson, K. D., D'Amato, C. J., Penney, J. B. & Young, A. B. (1988) *Proc. Natl. Acad. Sci. USA* **85,** 5733–5737.
28. Yohrling, G. J., IV, Jiang, G. C., DeJohn, M. M., Miller, D. W., Young, A. B., Vrana, K. E. & Cha, J. H. (2003) *Brain Res. Mol. Brain Res.* **119,** 28–36.
29. Gutekunst, C. A., Li, S. H., Yi, H., Mulroy, J. S., Kuemmerle, S., Jones, R., Rye, D., Ferrante, R. J., Hersch, S. M. & Li, X. J. (1999) *J. Neurosci.* **19,** 2522–2534.
30. Menalled, L. B. & Chesselet, M. F. (2002) *Trends Pharmacol. Sci.* **23,** 32–39.
31. Menalled, L. B., Sison, J. D., Wu, Y., Olivieri, M., Li, X. J., Li, H., Zeitlin, S. & Chesselet, M. F. (2002) *J. Neurosci.* **22,** 8266–8276.
32. Menalled, L. B., Sison, J. D., Dragatsis, I., Zeitlin, S. & Chesselet, M. F. (2003) *J. Comp. Neurol.* **465,** 11–26.
33. Bates, G. P., Mangiarini, L. & Davies, S. W. (1998) *Brain Pathol.* **8,** 699–714.
34. Nucifora, F. C., Jr., Sasaki, M., Peters, M. F., Huang, H., Cooper, J. K., Yamada, M., Takahashi, H., Tsuji, S., Troncoso, J., Dawson, V. L., *et al.* (2001) *Science* **291,** 2423–2428.
35. Jiang, H., Nucifora, F. C., Jr., Ross, C. A. & DeFranco, D. B. (2003) *Hum. Mol. Genet.* **12,** 1–12.
36. Holmberg, C. I., Staniszewski, K. E., Mensah, K. N., Matouschek, A. & Morimoto, R. I. (2004) *EMBO J.* **23,** 4307–4318.
37. Arrasate, M., Mitra, S., Schweitzer, E. S., Segal, M. R. & Finkbeiner, S. (2004) *Nature* **431,** 805–810.
38. Reynolds, D. S., Carter, R. J. & Morton, A. J. (1998) *J. Neurosci.* **18,** 10116–10127.
39. Maragos, W. F., Jakel, R. J., Pang, Z. & Geddes, J. W. (1998) *Exp. Neurol.* **154,** 637–644.
40. Bowyer, J. F., Clausing, P., Schmued, L., Davies, D. L., Binienda, Z., Newport, G. D., Scallet, A. C. & Slikker, W., Jr. (1996) *Brain Res.* **712,** 221–229.
41. Cyr, M., Beaulieu, J. M., Laakso, A., Sotnikova, T. D., Yao, W. D., Bohn, L. M., Gainetdinov, R. R. & Caron, M. G. (2003) *Proc. Natl. Acad. Sci. USA* **100,** 11035–11040.
42. Petersen, A., Larsen, K. E., Behr, G. G., Romero, N., Przedborski, S., Brundin, P. & Sulzer, D. (2001) *Hum. Mol. Genet.* **10,** 1243–1254.
43. Myers, R. H., Sax, D. S., Koroshetz, W. J., Mastromauro, C., Cupples, L. A., Kiely, D. K., Pettengill, F. K. & Bird, E. D. (1991) *Arch. Neurol. (Chicago)* **48,** 800–804.
44. Feigin, A., Kieburtz, K., Bordwell, K., Como, P., Steinberg, K., Sotack, J., Zimmerman, C., Hickey, C., Orme, C. & Shoulson, I. (1995) *Movement Disord.* **10,** 211–214.

NEUROSCIENCE